Macromolecules

Article

pubs.acs.org/Macromolecules

Effect of Rubber Polarity on Cluster Formation in Rubbers Cross-Linked with Diels–Alder Chemistry

L. M. Polgar,[†,‡] E. Hagting,[†] P. Raffa,[†] M. Mauri,[§] R. Simonutti,[§] F. Picchioni,*[,†,‡] and M. van Duin[†,∥]

[†]Department of Chemical Engineering, University of Groningen, Nijenborgh 4, 9747 AG Groningen, The Netherlands

[‡]Dutch Polymer Institute, P.O. Box 902, 5600 AX Eindhoven, The Netherlands

[§]Department of Materials Science, , University of Milano-Bicocca, Via R. Cozzi 55, 20125 Milano, Italy

[∥]ARLANXEO Performance Elastomers, Keltan R&D, P.O. Box 1130, 6160 BC Geleen, The Netherlands

Supporting Information

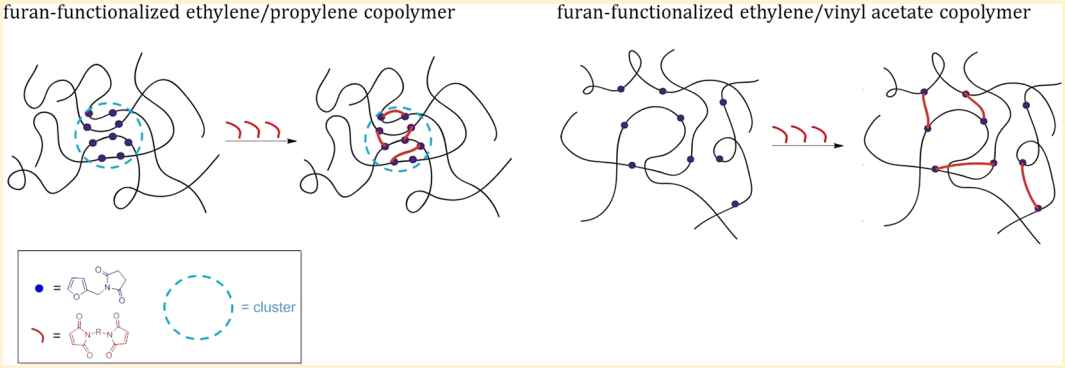

ABSTRACT: Diels–Alder chemistry has been used for the thermoreversible cross-linking of furan-functionalized ethylene/propylene (EPM) and ethylene/vinyl acetate (EVM) rubbers. Both furan-functionalized elastomers were successfully cross-linked with bismaleimide to yield products with a similar cross-link density. NMR relaxometry and SAXS measurements both show that the apolar EPM-*g*-furan precursor contains phase-separated polar clusters and that cross-linking with polar bismaleimide occurs in these clusters. The heterogeneously cross-linked network of EPM-*g*-furan contrasts with the homogeneous network in the polar EVM-*g*-furan. The heterogeneous character of the cross-links in EPM-*g*-furan results in a relatively high Young's modulus, whereas the more uniform cross-linking in EVM-*g*-furan results in a higher tensile strength and elongation at break.

1. INTRODUCTION

Rubbers can be divided into two classes, based on the amount of unsaturation in their polymer backbone. The most reactive elastomers, such as natural rubber, polyisoprene, and polybutadiene rubber, have a high level of unsaturation in their backbone. Elastomers with no unsaturation in the polymer chain, including ethylene/propylene rubber (EPM) and ethylene/vinyl acetate rubber (EVM), are relatively inert. Elastomers in the latter class distinguish themselves by their outstanding resistance to ozone, weathering, and high temperature.[1]

Both EPM and EVM copolymers have a very flexible polymer backbone with a high entanglement density, hardly or no crystallinity, and a relatively low glass transition temperature, which makes them soft and rubbery at room temperature. The major difference between EPM and EVM is their polarity. EPM is a hydrocarbon elastomer, containing only carbon and hydrogen atoms, and thus has a relatively low polarity. The large amount of vinyl acetate in EVM, on the other hand, results in a relatively high polarity. Both EPM copolymers with 40–55 wt % ethylene and EVM copolymers with 15–45 wt % ethylene are fully amorphous at room temperature due to the random copolymerization of ethylene with propylene or vinyl acetate, respectively, and the consequent absence of long ethylene (or vinyl acetate sequences).

Rubbers are typically cross-linked to achieve maximum elasticity and strength. Unfortunately, chemical cross-linking prohibits processing in the melt and, thus, prevents recycling of these materials. Current societal trends toward the limitation of waste and the need for more sustainable materials have increased the interest in and the appeal of reversible cross-linking of rubbers.[2−6] Thermoreversible cross-linking of maleated EPM and EVM rubbers modified with furfurylamine (FFA) has successfully been performed using the thermoreversible furan/maleimide Diels–Alder (DA) reaction (Scheme 1).[2,7]

There are strong indications that the grafting of maleic anhydride (MA) groups onto EPM results in MA grafts in a close proximity of each other along the polymer chain.[8] This is the result of intramolecular hydrogen transfer after the

Received: July 24, 2017
Revised: October 2, 2017
Published: November 7, 2017

DOI: 10.1021/acs.macromol.7b01541
Macromolecules 2017, 50, 8955–8964

Scheme 1. Furan Functionalization of Maleated EPM and EVM Rubber and Subsequent Thermoreversible Cross-Linking with Bismaleimide via (Retro) DA Chemistry

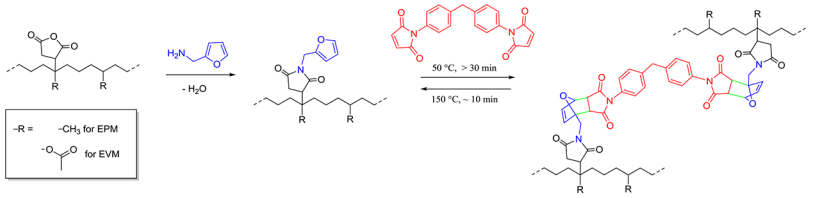

attachment of the first MA molecule to the EPM chain and is enhanced by the poor solubility of the polar MA in the apolar EPM rubber. Heterogeneity also exists on a supramolecular level in the maleated EPM as a result of phase separation of polar grafted MA groups from the apolar EPM matrix, resulting in MA-*graft*-rich clusters.[8,9] It is assumed that these clusters are maintained upon functionalization with polar FFA and that the polar BM cross-linker will preferably dissolve in these polar clusters. As a result, most DA cross-linking is expected to take place in these clusters, resulting in a heterogeneously cross-linked EPM rubber. EVM rubber is more polar; thus, there is probably little, if any at all, driving force for phase separation of polar MA grafts in maleated EVM. BM cross-linking of EVM-*g*-furan is therefore expected to result in a more homogeneously cross-linked rubber than the EPM-*g*-furan. Phase-separated clusters are known to be present in ionomeric rubbers.[10] The ionic groups generally segregate into multiplets, which in their turn form polar clusters.[11−14] The presence of such ionic clusters not only impart rubber conductivity, but the shape and degree of clustering also have a strong influence on the rubber material properties.[12,15,16] It is then conceivable that such influence will also be present for thermally reversible networks.

As a consequence of the above, the goal of this work is to study the presence of polar clusters and the effect of the network heterogeneity on the material properties of thermoreversibly BM cross-linked, apolar EPM and polar EVM. The expected heterogeneous network of BM cross-linked EPM may have different structure−property correlations compared to the BM cross-linked EVM. Amorphous elastomeric materials were used to avoid any complicating effects of crystallinity.

2. EXPERIMENTAL SECTION

2.1. Materials. The reference ethylene/propylene copolymer (EPM, Keltan 1500R, 49 wt % ethylene) and ethylene/vinyl acetate copolymer (EVM, Levamelt 700, 30 wt % ethylene, M_n = 35 kg/mol, PDI = 9) and the analogous, maleated EPM (EPM-*g*-MA, Keltan DE5005, 48 wt % ethylene, 50 wt % propylene, 2.1 wt % MA) and maleated EVM (EVM-*g*-MA, 30 wt % ethylene, 69 wt % vinyl acetate, 1.4 wt % MA) were kindly provided by ARLANXEO Performance Elastomers. The EPM-*g*-MA and EVM-*g*-MA precursors were dried in a vacuum oven at 175 °C for 1 h to convert any diacid present into the cyclic anhydride.[2,17] Furfurylamine (FFA, Sigma-Aldrich, ≥99%) was freshly distillated before use. 1,1-(Methylenedi-4,1-phenylene)-bismaleimide (BM, 95%), octadecyl-1-(3,5-di-*tert*-butyl-4-hydroxyphenyl)propionate (99%), dicumyl peroxide (DCP, 98%), tetrahydrofuran (THF, >99.9%), toluene (99.8%), decalin (mixture of cis and trans, 98%), and acetone (>99.5%) were all purchased from Sigma-Aldrich and used as received as reversible cross-linker, antioxidant, peroxide cross-linker, and solvents, respectively.

2.2. Methods. *2.2.1. Furan Functionalization of EPM-g-MA and EVM-g-MA.* 15 g of EPM-*g*-MA or EVM-*g*-MA rubber was dissolved in 150 mL of THF, after which 3 mol equiv of FFA (with respect to MA: 2.1 wt % in EPM-*g*-MA and 1.4 wt % in EVM-*g*-MA) was added. The reaction mixture was stirred at room temperature for 5 h in a closed system and, subsequently, precipitated into a 7-fold amount of demineralized water under stirring. The furan-functionalized polymer (EPM-*g*-furan or EVM-*g*-furan) was obtained as white threads. The polymer product was washed thoroughly with acetone to remove any unreacted FFA and dried under vacuum at 50 °C up to constant weight. Finally, the intermediate amide−acid was compression-molded at 175 °C and 100 bar for 15 min to ensure complete conversion to the cyclic imide.

2.2.2. Diels−Alder Cross-Linking of EPM-g-Furan and EVM-g-Furan. 10 g of EPM-*g*-furan or EVM-*g*-furan rubber was dissolved in 100 mL of THF, to which 1000 ppm phenolic antioxidant and 0.50 mol equiv of BM (with respect to the furan content) were added. When a homogeneous solution was obtained, the majority of the solvent was evaporated in the fume hood by blowing air over sample. The residual solvent was removed in a vacuum oven at 50 °C. Sample bars of the brownish mixtures were obtained by preheating the materials in a mold at 140 °C for 5 min and compression-molding them at 140 °C and 100 bar for 30 min.

2.2.3. Peroxide Curing of EPM and EVM. 26 g of EPM or EVM rubber was mixed with the DCP peroxide in an internal mixer (Brabender Messenkneder, Type W 30 EHT) at 50 rpm and 50 °C (75% fill factor). After homogenizing the gum rubber for 4 min, 2.0 phr of DCP was added, and after an additional 6 min of mixing, the mixture was collected. Subsequent vulcanization of the obtained mixtures was performed by preheating the samples in a mold at 160 °C for 5 min and compression-molding them at 160 °C and 50 bar for 35 min.

2.3. Characterization. Gel permeation chromatography (GPC) was performed using triple detection with refractive index, viscosity, and light scattering detectors, i.e., a Viscotek Ralls detector, a Viscotek viscometer Model H502, and a Shodex RI-71 refractive index detector, respectively. The separation was carried out using a guard column (PL-gel 5 μm Guard, 50 mm) and two columns (PL-gel 5 μm MIXED-C, 300 mm) from Agilent Technologies at 30 °C. THF (99+%), stabilized with butylated hydroxytoluene, was used as the eluent at a flow rate of 1.0 mL/min. The samples (∼2 mg/mL) were filtered over a 0.45 μm PTFE filter prior to injection. Four GPC measurements were performed on each sample. Data acquisition and calculations were performed using Viscotek OmniSec software version 4.6.1, using a refractive index increment (d*n*/d*c*) of 0.052. Molecular weights were determined using a universal calibration curve, generated from narrow polydispersity polystyrene standards (Agilent and Polymer Laboratories).

Elemental analysis (EA) of the rubber products for the elements N, C, and H was performed on a Euro EA elemental analyzer after thorough extraction of unreacted components and subsequent drying. The O content was calculated via the mass balance. The number of furan groups per chain for the furan-containing rubbers (#/chain) was calculated from M_n and the determined N content, according to a reported procedure.[2,7] The conversion of the BM cross-linking of EPM-*g*-furan and EVM-*g*-furan was determined in a similar fashion and can be used to determine the cross-link density $[XLD]_{ea}$.

The cross-link density $[XLD]_{es}$ was determined from equilibrium swelling experiments with decalin for EPM and with toluene for EVM. Rubber samples (approximately 500 mg) were weighed in 20 mL vials (W_0) and immersed in 15 mL of solvent until equilibrium swelling was reached (3 days). The sample was then weighed after removing the solvent on the surface with a tissue (W_1) and was finally dried in a vacuum oven at 110 °C until a constant weight was reached (W_2). The

DOI: 10.1021/acs.macromol.7b01541
Macromolecules 2017, 50, 8955−8964

gel content of the gum rubber samples is defined as $(W_2/W_0) \times 100\%$. The cross-link density was calculated from the weights of the swollen and dried rubber samples using the Flory–Rehner equation:[18−20]

$$[\mathrm{XLD}]_{es} = \frac{\ln(1 - V_R) + V_R + \chi V_R^{\,2}}{2V_S(0.5V_R - V_R^{\,1/3})} \quad \text{with } V_R = \frac{W_2}{W_2 + (W_1 - W_2)\frac{\rho_R}{\rho_S}} \tag{1}$$

where V_R is the volume fraction of rubber in swollen sample, V_S is the molar volume of solvent (154.3 and 106.3 mL/mol for decalin and toluene, respectively), χ is the interaction parameter (decalin/EPM: $0.121 + 0.278V_R$;[21] toluene/EVM: 0.133[18,19]), and ρ_R and ρ_S are the density of rubber (EPM: 0.860 g/mL; EVM: 0.930 g/mL) and solvent (decalin: 0.896 g/mL; toluene: 0.870 g/mL), respectively.

The cross-link density $[\mathrm{XLD}]_{ss}$ was determined from the stress–strain curves via the Mooney–Rivlin approach (eq 2).[22−25] Using the values of stress versus strain of a rubber sample obtained during tensile testing, one can obtain a linear proportionality between $\frac{\sigma}{2(\lambda - \lambda^{-2})}$ versus $1/\lambda$, from which the parameters C_1 and C_2 can be determined. The cross-link density is subsequently calculated from C_1 (eq 3).[23]

$$\sigma = 2\left(C_1 + \frac{C_2}{\lambda}\right)\left(\lambda - \frac{1}{\lambda^2}\right) \quad \text{with } \lambda = 1 + X\varepsilon \tag{2}$$

$$[\mathrm{XLD}]_{ss} = \frac{2C_1}{k_B T} \tag{3}$$

where σ is the true stress measured in the strained state, C_1 and C_2 are characteristic Mooney–Rivlin parameters of cross-linked rubber, representing effects of chemical cross-links and entanglements, respectively, λ is the extension ratio, X is the strain amplification factor defined as $\sigma E_0/\varepsilon$ ($X = 1$ for gum rubber), ε is the engineering strain, k_B is the Boltzmann constant (1.38×10^{-23} m^2 kg s^{-2} K^{-1}), and T is the temperature (in K).

The polymer chain dynamics was probed by performing time domain ^{1}H NMR (TD-NMR) with a Bruker Minispec MQ20 operating at 0.5 T static magnetic field corresponding to a proton resonance of 19.65 MHz. To measure the transverse relaxation of the elastomers, the Hahn echo pulse sequence was implemented.[26] Multiple-quantum (MQ) experiments were performed with a version of the Baum–Pines pulse sequence optimized for the TD-NMR setup by the addition of refocusing π pulses to increase stability at longer times.[27] The 90° pulse length was between 2.75 and 3 μs, the phase switching time was around 2.1 μs, and the receiver dead time was set at 14 μs. Most experiments were accumulated with more than 128 scans. Recycle delays of 1–2 s ensured full magnetization recovery between scans. Since mobility resolution is enhanced by higher temperature, the experiments were performed at 80 °C, the highest temperature for which the total experimental time was expected not to significantly reverse the cross-linking reaction.[28] This is crucial for MQ experiments, which required 4 h each and were also performed at 80 °C.

A single T_2 exponential was used to fit the complex transverse relaxation curves, yielding an average estimate of the chain mobility in each sample at each temperature, while a three-component model was also used to separate the contributions from the different components of the rubber network (eq 4).

$$\frac{I}{I_0} = A\exp\left\{-\frac{9}{40}D_{res}^{\,2}t^2\right\} + B\exp\left\{-\frac{t}{T_{2B}}\right\} + C\exp\left\{-\frac{t}{T_{2C}}\right\} \tag{4}$$

where I/I_0 is the FID intensity as a function of time normalized against the intensity at time 0, while A, B, and C are pre-exponential coefficients corresponding to specific population of chains in the network, D_{res} is the residual dipolar coupling, and T_{2B} and T_{2C} are characteristic relaxation times for the chain population B and C, respectively. In this model a rubber network is composed of three populations: first, a population of chains that are part of the rubbery network for which the relaxation is mostly due to the residual dipolar interactions and is thus represented by a Gaussian function; second, a population of loosely cross-linked chains for which the NMR signal decays exponentially with the characteristic time T_{2B}; third, a population of slowly relaxing protons with a high conformational freedom, such as chain ends and the sol fraction.[29]

The relaxation time is monotonically reduced by mobility constraints and, thus, decreases with an increasing density of both entanglements and cross-links. This relationship is modulated by the flexibility of the polymer chain and, thus, requires a precise calibration for each specific polymer.[30] Therefore, it is not possible to directly compare the T_2 values of the different polymers, since the T_g values of EVM(-*g*-furan) and EPM(-*g*-furan) are very different (−10 °C vs −50 °C).[7] We instead concentrated on the relaxometric variation between the EPM-*g*-furan and EVM-*g*-furan samples and their BM cross-linked counterparts in order to detect changes as a result of cross-linking. Chain dynamics was also studied using pulse sequences that stimulate and measure multiple quantum coherences (MQ) as recently developed for the study of cross-linked elastomers,[31] including EPDM.[32] The conceptual base of the technique is the measurement of ^{1}H residual dipolar coupling (D_{res}), an interaction between protons pertaining to different polymer chains through space. D_{res} is averaged to 0 in the case of fast isotropic molecular motion but is directly proportional to the density of cross-links in the case of polymer networks (eq 5).

$$D_{res} = D_{eff}\frac{3}{5N} \tag{5}$$

where D_{eff} is the static interaction parameter dependent on the polymer and N is the number of segments between cross-links. In particular, the modified Baum–Pines sequence presented above produces a buildup of the DQ with increasing excitation time, whence D_{res} can be extracted using appropriate functions, the most used of which is the Abragam-like (A-l).[27] In real networks, the segments between cross-links are not univocally determined, and thus the DQ buildup must be fitted considering the distribution of N and, thus, D_{res}. Here, data analysis was performed with Tichonov regularization[33] using an A-l kernel function.

Small-angle X-ray scattering (SAXS) measurements were performed using an advanced Nano-Star SAXS setup, i.e., a homemade assembly of a NanoStar camera and a Microstar X-ray generator from Bruker AX-S.[34,35] The collimation line between the rotating X-ray generator and the camera consists of a multilayer optics Montel-P from Incoatec and three pinholes of 0.5, 0.3, and 0.5 mm in diameter from Rigaku, spaced at distances of ca. 14, 40, and 62 cm, respectively, from the middle of the optics unit. Passing through the optics, the primary beam is monochromized for Cu Kα radiation (λ = 1.542 Å) and simultaneously collimated to obtain a low-divergent beam. Both the optics and the collimation line with the first and the second pinholes are evacuated. The third pinhole, located in the sample chamber of the NanoStar camera, is in air. The SAXS intensity profiles were acquired at room temperature, running the X-ray generator at 45 kV and 60 mA, affording a primary X-ray beam flux at the sample position of 8×10^8 photons/(s mm^2) and a beam diameter of 0.4 mm. The sample-to-detector distance was set to 105 cm, and data were collected for 3 min per rubber sample.

The Yarusso and Cooper (YC) model[36] is used to interpret the SAXS profiles, yielding the characteristics of any clusters.[9,37] This hard-sphere model describes clusters as spherical domains with radius R_1, surrounded by a polymeric layer with restricted-mobility with radius R_2 (Figure 1).[31] The domains are arranged in a liquidlike order with a distance of closest approach of $2R_2$. The average volume of one scattering domain is defined as $V_p = 4/3\pi R_1^{\,3}$. Finally, $\Delta\rho$ is defined as the difference in electron density between the scattering domain and the polymer matrix.[17,36]

Tensile tests were performed on an Instron 5565 with a clamp length of 15 mm, according to the ASTM D4-112 standard. Strain rates of 500 and 5 mm/min were applied. Test samples with a width of 4.5 ± 0.1 mm and a thickness of 1.0 ± 0.1 mm were prepared by compression molding. For each measurement 10 samples were tested, and the two outliers with the highest and the lowest values were

DOI: 10.1021/acs.macromol.7b01541
Macromolecules 2017, 50, 8955−8964

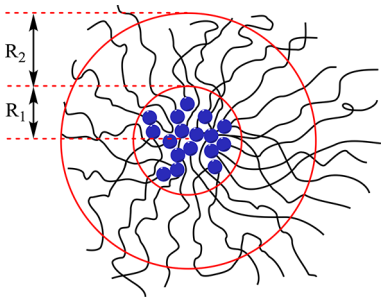

Figure 1. Schematic representation of a spherical, MA-*graft*-rich domain in EPM-*g*-MA with R_1 the radius of the domain and R_2 the radius of the polymeric restricted-mobility layer surrounding this domain.

excluded. Numerical data presented are averages of the other eight tests. The median stress−strain curve was selected to represent the entire series of a sample. Hardness Shore A was measured using a Bareiss durometer, according to the ASTM D2240 standard. Cylindrical test samples with a thickness of 6.0 ± 0.1 mm and a diameter of 13.0 ± 0.1 mm were prepared by compression molding. Average values were obtained from 10 measurements. Compression set tests were performed according to the ASTM D931 standard, using a homemade device and the cylindrical samples of 6 ± 0.1 mm thickness. The samples were compressed to 75% of their original thickness for 70 h at room temperature and then relaxed for 30 min at 50 °C. Compression molding of all test samples was performed on a Taunus Ton Technik V8UP150A press for 30 min at 140 °C and 100 bar for 30 min.

3. RESULTS AND DISCUSSION

3.1. Molecular Characterization. The reference EPM and EVM rubbers and their maleated and furan-functionalized analogues were characterized by GPC and EA (Table 1). While the PDI of EPM is similar to that of EPM-*g*-MA and EPM-*g*-furan, the PDI of EVM increases upon maleation, suggesting degradation and branching via combination of intermediate EVM macroradicals. The conversion of both maleated elastomers to the imide products is high (>90%).

The relatively high gel contents approaching 100% for all samples (Table 2) indicate that all chains are part of the rubber network. The cross-link densities of the BM cross-linked and DCP cured EPM and EVM products were determined by EA, equilibrium swelling, and stress−strain testing (Table 2). Since the cross-link density is one of the main variables affecting the properties of vulcanized rubbers,[38] the similar cross-link density ($\pm 0.1 \times 10^{-4}$ mol/mL) of the BM cross-linked EPM-*g*-furan and EVM-*g*-furan allows for a fair comparison of the material properties of these samples with each other and with their DCP cured references. For both BM cross-linked elastomers, the cross-link density determined from EA corresponds fairly to the one determined by equilibrium swelling. The cross-link density determined from the stress−strain curve, however, is significantly larger than those determined from EA and equilibrium swelling. This may be because elemental analysis is a direct chemical method, swelling is an equilibrium measurement, and the tensile tests are time dependent. The cross-link density obtained from stress−strain curves includes both the true chemical cross-links and the permanently trapped chain entanglements. Some entanglements will disentangle during equilibrium swelling,[39−41] which is not possible on the short time scale of the tensile experiments and will therefore significantly contribute to $[XLD]_{ss}$.

The difference between the cross-link densities determined by the different methods appears to be relatively small for the BM cross-linked EPM-*g*-furan. This may be related to the heterogeneity of the cross-linked network. If the cross-linking points are more sparsely divided throughout the rubber matrix, they are less capable of trapping entanglements than a more homogeneously cross-linked network such as the BM cross-linked EVM-*g*-furan or the DCP cured EPM and EVM. As a result, a heterogeneously cross-linked network with a certain amount of cross-links may appear to be less cross-linked than a homogeneously cross-linked network with the same number of cross-links.[42] The reversible character of the BM cross-linking may add to the observed discrepancies, as during a swell test the polymer is left in solution for 3 days during which the dynamic, reversible cross-links may open and close, allowing for the disentanglement of previously trapped entanglements.

3.2. Network Mobility. Fitting the TD-NMR relaxation of EPM and EVM samples with a single exponent provides an acceptable fitting ($\sigma_{T_2} \sim 0.01$ ms) of the initial decay and higher residuals at higher echo times (Table 3). This fitting does not account for the slow relaxing tail due to the presence of sol or chain ends (Figure S1). The absence of an evidently Gaussian decay in the initial region indicates that the chemical cross-link density is close to the entanglement density, which corresponds with previously reported estimates of the entanglement density at $(1.8-2.2) \times 10^{-4}$ mol/mL for both polymers. Fitting with three components closely resembles the experimental curve and confirms that the relaxation is dominated by the mono-exponential population of B that accounts for 70%−80% of the curve but also explicitly singles out the long relaxing component C as well as a the strongly cross-linked component A. The D_{res} appear to be inversely proportional to the polymer chain mobility, which indicates a qualitative difference between the EVM and EPM samples. The coupling parameters for the EPM samples are much higher, hinting at strongly bound polar clusters (at the limits of phase separation), while the lower values for the EVM samples are compatible with local

Table 1. Characterization of Rubber Samples

	M_n (kg/mol)	PDI	elemental content (wt %) N, C, H → O	conversion (%)	#/chain[a]
EPM	53 ± 4	2.0 ± 0.2	<0.01, 86.67, 13.33 → 0.0		
EVM	35 ± 3	9 ± 0.7	<0.01, 64.41, 9.19 → 26.4		
EPM-*g*-MA	54 ± 4	2.0 ± 0.2	<0.01, 84.70, 14.30 → 1.0		11[b]
EVM-*g*-MA	31 ± 2	17 ± 1.3	<0.01, 65.40, 9.61 → 25.0		4.4[b]
EPM-*g*-furan	55 ± 5	2.1 ± 0.2	0.27, 84.80, 14.20 → 0.7	93	10[c]
EVM-*g*-furan	31 ± 3	17 ± 1.2	0.20, 66.37, 9.52 → 23.9	98	4.3[c]

[a]An estimate of the average number of functional groups on each polymer. [b]Based on MA content. [c]Based on nitrogen content as determined from EA results.

DOI: 10.1021/acs.macromol.7b01541
Macromolecules 2017, 50, 8955−8964

Table 2. Cross-Link Densities As Determined from Elemental Analysis, Equilibrium Swelling, and Tensile Testing

	elemental content (wt %) N, C, H → O	gel content (%)	$[XLD]_{ea}$ (10^{-4} mol/mL)	$[XLD]_{es}$ (10^{-4} mol/mL)	$[XLD]_{ss}$ (10^{-4} mol/mL)
BM cross-linked EPM-*g*-furan	0.36, 83.65, 12.52 → 3.5	97	1.1	0.73 ± 0.1	1.1 ± 0.2
BM cross-linked EVM-*g*-furan	0.42, 65.16, 9.34 → 25.1	95	1.0	0.88 ± 0.1	1.4 ± 0.2
DCP cured EPM	<0.01, 85.72, 12.95 → 1.3	99		0.89 ± 0.2	1.5 ± 0.3
DCP cured EVM	<0.01, 63.78, 9.00 → 27.2	98		0.84 ± 0.1	1.1 ± 0.2

Table 3. Single- and Three-Component Fitting Parameters for ^{1}H NMR Transverse Relaxation Curves Acquired at 80 °C

		three-component fit					
	av T_2 (ms)	A (%)	D_{res} (Hz)	B (%)	T_{2B} (ms)	C (%)	T_{2C} (ms)
EPM-*g*-furan	0.93 ± 0.02	8.6	650 ± 10	81.8	0.81 ± 0.02	9.6	7.11 ± 0.10
EVM-*g*-furan	0.88 ± 0.02	12.8	160 ± 10	76.2	0.53 ± 0.01	11.1	4.10 ± 0.05
BM cross-linked EPM-*g*-furan	0.99 ± 0.02	9.4	570 ± 10	81.2	0.87 ± 0.02	9.4	6.70 ± 0.10
BM cross-linked EVM-*g*-furan	0.80 ± 0.02	14.7	200 ± 10	73.1	0.45 ± 0.01	12.3	3.35 ± 0.05

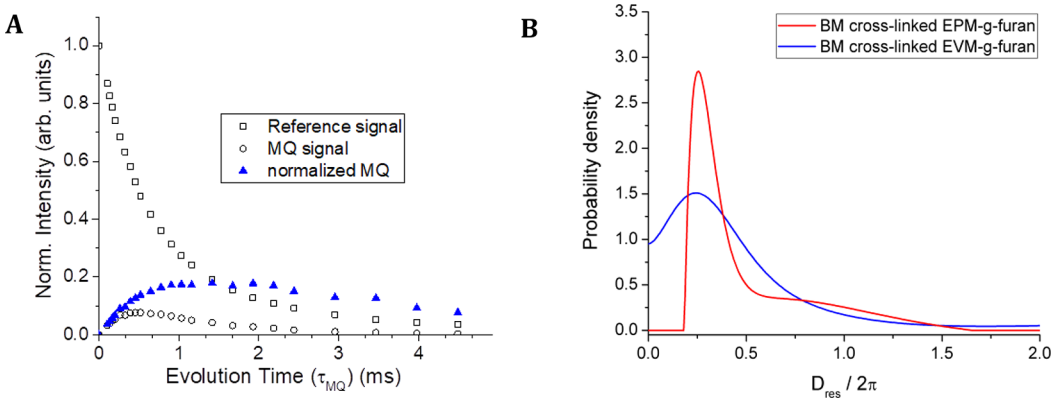

Figure 2. (A) TD-NMR MQ buildup and reference signals for BM cross-linked EVM-*g*-furan. The uncorrected, normalized MQ curve is highlighted using solid dots. (B) Residual dipolar coupling distribution obtained by fitting the corrected MQ curves for BM cross-linked EPM-*g*-furan and EVM-*g*-furan.

heterogeneities with a motional regime that is only slightly different from the surrounding B population.

Interestingly, the differences between the cross-linked and non-cross-linked samples are not that large, since even the non-cross-linked samples present a fraction of strongly dipolar coupled chains (A), and all values for the populations and relaxation times are similar. It seems as if the structuration within the polymer is already set by the polarity, while the additional cross-linking, which by elemental analysis can be estimated as smaller than the intrinsic entanglement density, acts as structural fixating agent. The only significant difference is that cross-linking in the homogeneous EVM system causes a decrease in the mobility of population B, thus reducing T_{2B}. Instead, the heterogeneous EPM system displays an increase of T_{2B}.

TD-NMR studies the polymer in its native state without stress or swelling and can, therefore, be used in addition to other methods used to determine the cross-link density. These NMR measurements indicate that BM cross-linking of EPM-*g*-furan occurs in a heterogeneous fashion. The increase in cross-link density due to the presence of BM reduces the T_2 relaxation time of the main component of the homogeneous EVM sample. However, a comparison between the corresponding EPM samples shows an increase of T_2 of the mobile phase, which is an indication that cross-linking is mostly taking place in the phase-separated, polar clusters.

3.3. Polar Clusters. Since TD-NMR can provide a direct measurement of the homogeneity of vulcanized rubbers, the relevant MQ-NMR sequences were used on the BM cross-linked samples (Figure 2). It must be noted that the normalized MQ NMR signal of both BM cross-linked rubber samples reaches a maximum value of 0.2, which is very far from the theoretical value of 0.5 for a fully cross-linked rubber. This relatively low value is in agreement with previous literature observations on EPM and EPDM rubbers.[32] It can be explained by the presence of fractions of loosely cross-linked regions and other protons that do not contribute to MQ coherence. To correct of this effect and allow the extraction of D_{res} distribution, a two-component exponential fitting of the long-time tail of the reference signal was performed. By subtracting this contribution from the reference signal, the corrected MQ signal reaches 0.5 and D_{res} distributions could be obtained by Tichonov regularization (Figure 2B). The cross-linked EVM-*g*-furan displays a wide distribution of residual dipolar couplings around a single value, while the cross-linked EPM-*g*-furan clearly has a bimodal distribution, with one population sharply centered around a low D_{res} value (≈250 Hz) and a long tail at higher couplings which is associated with the presence of polar clusters.

Different polymers have different proportionality between D_{res} and XLD (eq 5). Still, internal analysis of the bimodal D_{res} curve associated with BM cross-linked EPM-*g*-furan can be

DOI: 10.1021/acs.macromol.7b01541
Macromolecules 2017, 50, 8955−8964

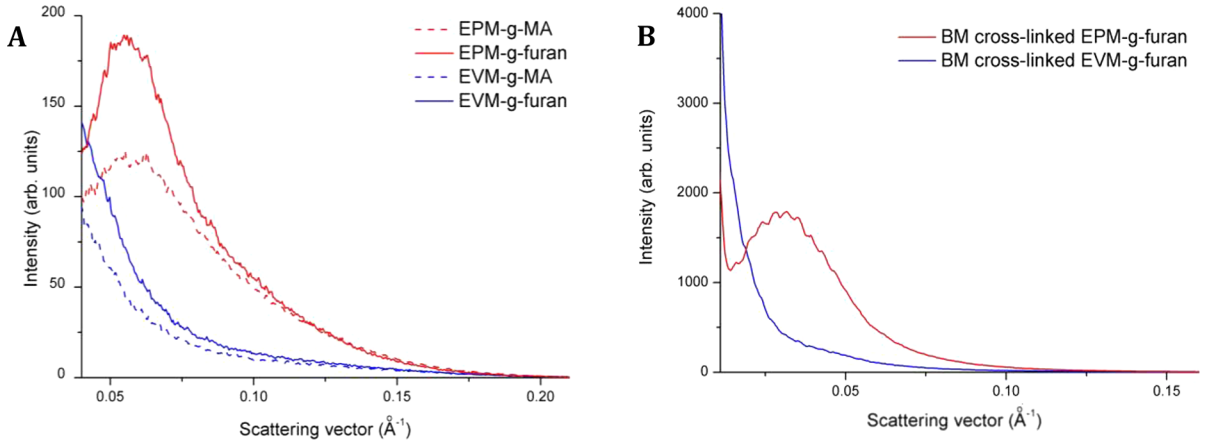

Figure 3. SAXS characterization of (A) MA- and furan-functionalized EPM and EVM and (B) BM cross-linked EPM-*g*-furan and EVM-*g*-furan.

performed. By considering the long tail as a second distribution centered around 900 Hz, it can be estimated that the polar clusters have a XLD around 3.5 times higher than the rest of the material.

SAXS measurements of the various (functionalized and/or cross-linked) EPM and EVM samples were performed to investigate the presence of polar clusters and their size and structure (Figure 3). The starting EPM and EVM rubbers are fully homogeneous, as no SAXS scattering is observed (not shown). For all functionalized and/or cross-linked EPM samples a scattering peak is observed in the SAXS profile, which implies that they all contain aggregates that differ in electron density from the polymer matrix. For EPM-*g*-MA and EPM-*g*-furan the scattering peak is observed at a scattering vector values (q) of 0.057 Å^{-1}, which is in good agreement with data reported before.[9,17] The broad scattering peak confirms the microphase separation of the grafted anhydride and furan groups into MA- and furan-graft rich domains, which is driven by the large polarity difference between the polar MA and furan grafts and the apolar EPM polymer backbone (the solubility parameters of EPM and EVM are 16 and 22 MPa$^{0.5}$, respectively, while those of MA, furan, and BM are 28, 27, and 24 MPa$^{0.5}$, respectively).[17] For EVM-*g*-MA and EVM-*g*-furan such a scattering peak is not observed, which confirms that the polar vinyl acetate in EVM impedes the formation of MA-graft rich clusters. Any fluctuation in motional dynamics detected by TD-NMR in the BM cross-linked EVM-*g*-furan is not strong enough to be associated with a variation in density as detected by SAXS.

While BM cross-linking of EPM-*g*-furan results in a significant increase in scattering intensity and a shift of the scattering peak to a lower q value of 0.03 Å^{-1}, SAXS scattering remains absent upon BM cross-linking of EVM-*g*-furan. The changes observed upon BM cross-linking of EPM-*g*-furan are associated with an increase in the cluster size and the Bragg spacing (d), which is the distance between the clusters according to $q = 2\pi/d$. The Bragg spacing increases from 11.2 to 20.9 nm upon cross-linking EPM-*g*-furan, implying that the polar clusters become less closely packed and increase in size. This increase is a result of the presence the added BM in the clusters and the nature of the strained bonds formed that by connecting the polar functional groups also push them apart from each other. The related SAXS peak is known to shift to lower q values upon such an increase in cluster size.[9,36,37]

The SAXS scattering observed for the functionalized and/or cross-linked EPM samples arises both from thermal, time-dependent fluctuations in cluster concentrations, as a result of Brownian motion (dynamic contributions), and from the heterogeneous distribution of cross-links (static contributions).[43] These dynamic and static scattering contributions were separated by subtracting the scattering intensity of the corresponding, non-cross-linked polymer, assuming the latter solely reflects the dynamic scattering contribution,[42] to obtain the Yarusso−Cooper fit parameters of the SAXS patterns of EPM-*g*-MA, EPM-*g*-furan, and BM cross-linked EPM-*g*-furan (Table 4).

Table 4. Fit Parameters of SAXS Patterns of Functionalized and/or Cross-Linked EPM ($R^2 > 0.99$)

sample	R_1 (Å)	R_2 (Å)	$R_2 - R_1$ (Å)	V_p (Å^3)	$\Delta\rho$ (e$^-$/Å^3)	d (Å)
EPM-*g*-MA	22.3	44.1	21.8	4.65×10^4	0.35	112
EPM-*g*-furan	23.9	47.9	24.0	5.72×10^4	0.28	120
BM cross-linked EPM-*g*-furan	43.2	77.9	34.7	3.38×10^5	0.47	209

An expected increase in cluster size R_1 is observed upon the furan-functionalization of EPM-*g*-MA. When all grafted polar groups are phase-separated from the EPM matrix, $\Delta\rho$ can provide information about the composition of the scattering particle.[9] Formation of DA cross-links in polar clusters results in a significant increase in the electron density because of the very high polarity of the BM cross-linker. This over-compensates the increased cluster volume and results in an increase in $\Delta\rho$. The thickness of the restricted-mobility layer ($R_1 - R_2$) also increases with the size of the polar clusters (R_1). In conclusion, SAXS shows the presence of polar clusters in (BM cross-linked) EPM-*g*-furan and their absence in (BM cross-linked) EVM-*g*-furan samples. This confirms that the cross-links are spatially more homogeneously distributed in BM cross-linked EVM-*g*-furan than in BM cross-linked EPM-*g*-furan.

3.4. Material Properties. The material properties of cross-linked rubbers are mainly influenced by their cross-link density. In this study, the cross-link densities of the BM cross-linked elastomers and of the DCP cured references are all roughly 8×10^{-5} mol/mL, thus enabling a fair comparison[43] and investigation of the network structure (as illustrated by the NMR relaxometry and SAXS measurements discussed above)

DOI: 10.1021/acs.macromol.7b01541
Macromolecules 2017, 50, 8955−8964

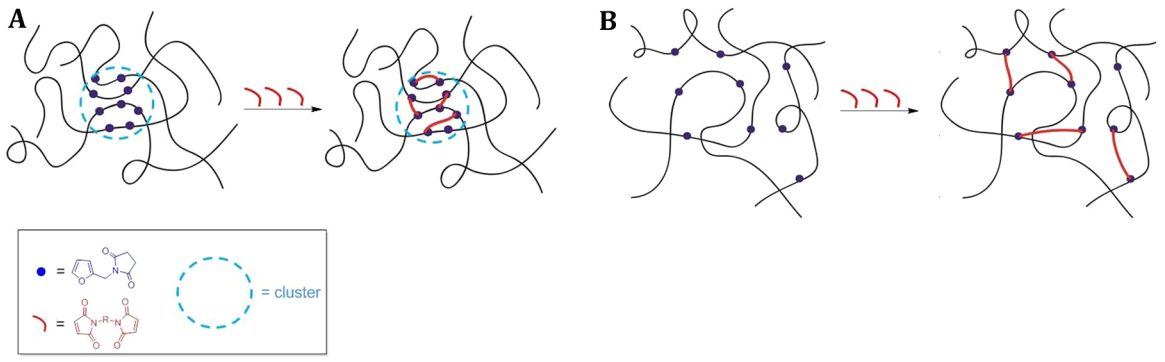

Figure 4. Schematic representation of (A) heterogeneously cross-linked EPM-*g*-furan and (B) homogeneously cross-linked EVM-*g*-furan.

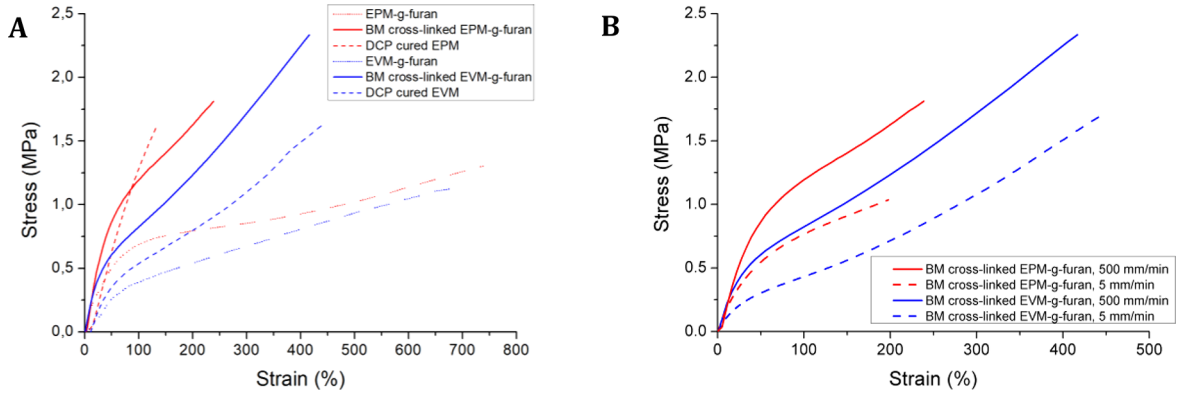

Figure 5. Median stress−strain curves of (A) EPM-*g*-furan and EVM-*g*-furan, their BM cross-linked products, and DCP cured EPM and EVM references at similar cross-link density at a strain rate of 500 mm/min and (B) BM cross-linked EPM-*g*-furan and EVM-*g*-furan at strain rates of 5 and 500 mm/min.

on the final properties, which constitutes a novel and crucial point of the present work. Indeed, the (BM cross-linked) EPM-*g*-furan samples used in this study are cross-linked in phase-separated domains. Their material properties will therefore also depend on the structure (network heterogeneity) and dynamics (the reversibility of the cross-links via the DA equilibrium reaction and the hopping of polar groups between clusters) of the microphase-separated domains (Figure 4). The cross-links are closely packed in these polar clusters and act cooperatively as a single cross-linked node with a low individual ability for elastic-energy storage.[42,44,45] In a network consisting of highly cross-linked zones embedded in a matrix of a less cross-linked polymer, stress will accumulate in these zones of elevated functionality.[50] On the contrary, a network with a uniform cross-link distribution will be able to transfer applied stress more efficiently so that all the chains in the network will bear an equal stress load. This has a relevant influence on the mechanical behavior as discussed below.

The stress−strain curves of the starting EPM-*g*-furan and EVM-*g*-furan samples are typical for non-cross-linked rubbers exerting very low stress upon stretching to extremely large extensions (Figure 5A). The initial slope of the stress−strain curve of EPM-*g*-furan (dashed red line) is somewhat steeper than that of EVM-*g*-furan (dashed blue line) because of the presence of polar clusters in the former, acting as physical cross-links on the time scale of tensile testing. The subsequent flattening of the curve upon further stretching the EPM-*g*-furan sample is then a result of the rupture of the physical interactions in these clusters. BM cross-linking of both rubbers (solid lines) results in the expected upswing of the tensile curves. The shape of the stress−strain curves of the DCP cured reference samples (dotted lines) are similar as both materials are homogeneously cross-linked. The EPM sample has an overall higher stress at the same strain than the EVM sample. This is also observed for the (BM cross-linked) EPM-*g*-furan and EVM-*g*-furan and must therefore also be influenced by the chemical structure and/or the molecular weight of the polymer backbone. The difference in shape between the stress−strain curves of the BM cross-linked EPM-*g*-furan and the DCP cured EPM, however, is a result of the polar domains in the former as the shape of the stress−strain curves of the BM cross-linked EVM-*g*-furan and DCP cured EVM are more similar to each other.

A qualitative comparison of the stress−strain curves of the BM cross-linked EPM-*g*-furan and EVM-*g*-furan at different strain rates (Figure 5B) may give some insight into the effect of the heterogeneity of the network (*vide supra*).[46] An increase of strain rate from 5 to 500 mm/min results in an increase in Young's modulus (from 2.3 to 2.9 MPa for EPM-*g*-furan and from 1.9 to 2.6 MPa for EVM-*g*-furan) and tensile strength (from 0.9 to 1.8 MPa for EPM-*g*-furan and from 1.6 to 2.3 MPa for EVM-*g*-furan), whereas the elongation at break is more or less unaffected. This stems probably from the relative comparison between the time scale of the tensile measurement and the kinetics of reversible network formation and rupture, with the measurement at 500 mm/min being too fast for a detailed appreciation of this network dynamics. At both strain rates of 5 and 500 mm/min, the BM cross-linked EPM-*g*-furan shows an initial accumulation of stress at low strain. Again, the stress localization in the cross-linked clusters eventually leads to

DOI: 10.1021/acs.macromol.7b01541
Macromolecules 2017, 50, 8955−8964

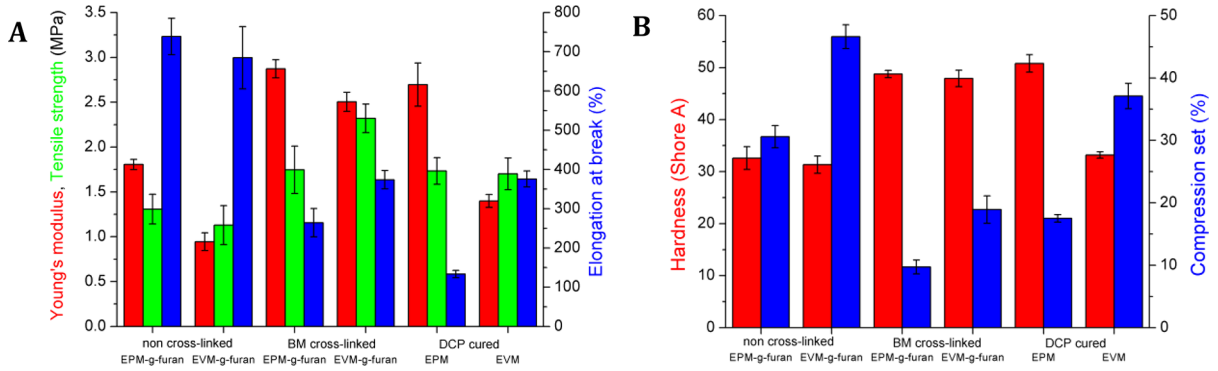

Figure 6. (A) Tensile properties and (B) hardness and compression set of EPM-*g*-furan and EVM-*g*-furan, corresponding BM cross-linked products, and DCP cured EPM and EVM references with similar cross-link densities. The error bars indicate ±1 standard deviation.

rupture of these clusters and/or the pull-out of some chains from the clusters, as is indicated by the flattening of the stress−strain curve to the same stress−strain slope as the BM cross-linked EVM-*g*-furan. The homogeneous distribution of cross-links in the BM cross-linked EVM-*g*-furan rubber results a more even distribution of the applied stress over the network and is evidenced by the initially less stiff response during extensional deformation and a more gradual breakage of the cross-links at higher strains.[47,48]

The observed increase in hardness, Young's modulus and tensile strength, and the decrease in elongation at break and compression set observed upon BM cross-linking of EPM-*g*-furan and EVM-*g*-furan (Figure 6) are typical for the cross-linking of rubber.[49−52] The same effect is observed upon peroxide curing of EPM and EVM. The starting EPM and EVM display a very low stress (~0.3 MPa) up to the maximum strain of the tensile test machine (curves not shown). The BM cross-linked EPM-*g*-furan has a higher hardness, Young's modulus and a lower tensile strength, elongation at break, and compression set than the BM cross-linked EVM-*g*-furan. This nicely confirms the hypothesis that the localized polar domains in the BM cross-linked EPM-*g*-furan act as (additional) physical network nodes. The Young's modulus and tensile strength of the BM cross-linked samples are larger than their DCP cured references, but the hardness and compression set are lower. This stems probably from the different time scales of these measurements as tensile properties are generally measured on a shorter time scale (on the order of few seconds) than hardness and compression set tests. The networks dynamics then allow for adaptation to the imposed stress over relatively large time scales of the latter.

The retro-DA reaction facilitates the breaking of cross-links upon imposing strain for both EPM-*g*-furan and EVM-*g*-furan. However, for the heterogeneously cross-linked EPM product a certain strain is also required to remove a furan-functional chain out of the phase-separated domains in which the cross-links reside. This explains the lower tensile strength, elongation at break, and the decreased effectiveness of the heterogeneously dispersed, cross-linked domains in the BM cross-linked EPM-*g*-furan with respect to the homogeneously BM cross-linked EVM-*g*-furan.[47] No significant effects were observed when considering the hardness, Young's modulus, and compression set. It must be stressed here that the observed differences between the material properties of the (BM cross-linked) EPM-*g*-furan and EVM-*g*-furan samples would have been even more evident if the molecular weights of the two elastomers were the same (50 kg/mol for EPM-*g*-furan versus 30 kg/mol for EVM-*g*-furan), since the yield stress typically increases with molecular weight as a result of the larger number of entanglements per polymer molecule.[53] This constitutes the subject of future investigation in our group.

Finally, previous recycling studies on the thermoreversible cross-linking of the same furan-containing EPM and EVM polymers showed 97, 90, 95, 86, and 107% versus 83, 89, 93, 74, and 73% retention for the hardness, Young's modulus, tensile strength, elongation at break, and compression set, respectively.[2,7] It was thus concluded that the retention of the material properties upon reprocessing in the melt is somewhat higher—actually almost ideal—for the BM cross-linked EPM-*g*-furan compared to the corresponding EVM-*g*-furan. Again, this difference is probably also related to the presence of polar clusters in EPM-*g*-furan as the products formed upon retro-DA de-cross-linking will stay in close vicinity to each other in the polar domains and thus will more easily recombine via the DA cross-linking reaction after melt processing.

4. CONCLUSIONS

Two maleated elastomers (EPM-*g*-MA and EVM-*g*-MA) were thermoreversibly cross-linked via Diels−Alder chemistry in a straightforward, two-step approach of furan-functionalization and subsequent bismaleimide cross-linking. TD-NMR and SAXS measurements show the presence of clusters in the apolar EPM elastomers and their absence in the polar EVM elastomers, indicating phase separation of the polar MA/furan groups in the former. DA cross-linking of EPM-*g*-furan with polar BM takes predominantly place in these polar clusters, resulting in a heterogeneously cross-linked network. Differences in material properties between the two cross-linked elastomers can be attributed to the homogeneity (or lack thereof) of the cross-linked networks, as they are compared at the same cross-link density. The heterogeneous character of the rubbery network in EPM-*g*-furan initially results in a relatively high modulus, whereas homogeneous cross-linking in EVM-*g*-furan results in a higher tensile strength and elongation at break.

■ ASSOCIATED CONTENT

Supporting Information

The Supporting Information is available free of charge on the ACS Publications website at DOI: 10.1021/acs.macromol.7b01541.

Figures S1−S3 (PDF)

DOI: 10.1021/acs.macromol.7b01541
Macromolecules 2017, 50, 8955−8964

AUTHOR INFORMATION

Corresponding Author

*E-mail f.picchioni@rug.nl (F.P.).

ORCID

R. Simonutti: 0000-0001-8093-517X

F. Picchioni: 0000-0002-8232-2083

Notes

The authors declare no competing financial interest.

ACKNOWLEDGMENTS

This study forms part of the research program of the Dutch Polymer Institute, project #749. Dr. Rainer Kalkofen (ARLANXEO Germany) is acknowledged for providing the (maleic anhydride containing) EVM samples.

REFERENCES

(1) Baranwal, K. C.; Stephens, H. L. *Basic Elastomer Technology*; American Chemical Society Rubber Devision: Akron, OH, 2001.

(2) Polgar, L. M.; van Duin, M.; Broekhuis, A. A.; Picchioni, F. The use of Diels-Alder chemistry for thermoreversible cross-linking of rubbers: the next step towards recycling of rubber products? *Macromolecules* **2015**, *48*, 7096−7105.

(3) Myhre, M.; MacKillop, D. A. Rubber recycling. *Rubber Chem. Technol.* **2002**, *75*, 429−474.

(4) van der Mee, M. A. J.; Goossens, J. G. P.; van Duin, M. Thermoreversible cross-linking of maleated ethylene/propylene copolymers with diamines and amino-alcohols. *Polymer* **2008**, *49*, 1239−1248.

(5) Imbernon, L.; Norvez, S. From landfilling to vitrimer chemistry in rubber life cycle. *Eur. Polym. J.* **2016**, *82*, 347−376.

(6) Li, L.; Kim, J. K. Thermoreversible Cross-Linking Maleic Anhydride Grafted Chlorobutyl Rubber with Hydrogen Bonds (Combined with Ionic Interactions). *Rubber Chem. Technol.* **2014**, *87*, 459−470.

(7) Polgar, L. M.; Hagting, E.; Koek, W. J.; van Duin, M.; Picchioni, F. Thermoreversible cross-linking of furan-containing ethylene/vinylacetate rubber with bismaleimide. *Polymers* **2017**, *9*, 81−13.

(8) van Duin, M. Grafting of polyolefins with maleic anhydride: Alchemy or technology? *Macromol. Symp.* **2003**, *202*, 1−10.

(9) Wouters, M. E. L.; Goossens, J. G. P.; Binsbergen, F. L. Morphology of neutralized low molecular weight maleated ethylene-propylene copolymers (MAn-g-EPM) as investigated by small-angle X-ray scattering. *Macromolecules* **2002**, *35*, 208−216.

(10) Hall, L. M.; Stevens, M. J.; Frischknecht, A. L. Effect of Polymer Architecture and Ionic Aggregation on the Scattering Peak in Model Ionomers. *Phys. Rev. Lett.* **2011**, *106*, 127801.

(11) Eisenberg, A. Clustering of ions in organic polymers. *Macromolecules* **1970**, *3*, 147−154.

(12) Eisenberg, A.; Kim, J. *Introduction to Ionomers*; John Wiley and Sons: Hoboken, NJ, 1998.

(13) Rigdahl, M.; Eisenberg, A. Viscoelastic Properties of Sulfonated Styrene Ionomers. *J. Polym. Sci., Polym. Phys. Ed.* **1981**, *19*, 1641−1654.

(14) Eisenberg, A.; Hird, B.; Moore, R. B. A New Multiplet-Cluster Model for the Morphology of Random Ionomers. *Macromolecules* **1990**, *23*, 4098−4107.

(15) Peng, R. D.; Zhou, H. W.; Wang, H. W.; Mishnaevsky, L., Jr. Modeling of nano-reinforced polymer composites: Microstructure effect on Young's modulus. *Comput. Mater. Sci.* **2012**, *60*, 19−31.

(16) Agrawal, A.; Perahia, D.; Grest, G. S. Clustering effects in ionic polymers: Molecular dynamics simulations. *Phy Rev. E* **2015**, *92*, 022601.

(17) van der Mee, M. A. J.; I'Abee, R. M. A.; Portale, G.; Goossens, J. G. P.; van Duin, M. Synthesis, structure, and properties of ionic thermoplastic elastomers based on maleated ethylene/propylene copolymers. *Macromolecules* **2008**, *41*, 5493−5501.

(18) Posadas, P.; Fernandez-Torres, A.; Chamorro, C.; Mora-Barrantes, I.; Rodriguez, A.; Gonzalez, L.; Valentin, J. L. Study on peroxide vulcanization thermodynamics of ethylenevinyl acetate copolymer rubber using 2,2,6,6,-tetramethylpiperidinyloxyl nitroxide. *Polym. Int.* **2013**, *62*, 909−918.

(19) Hirschl, C.; Biebl-Rydlo, M.; DeBiasio, M.; Muehleisen, W.; Neumaier, L.; Scherf, W.; Oreski, G.; Eder, G.; Chernev, B.; Schwab, W.; Kraft, M. Determining the degree of crosslinking of ethylene vinyl acetate photovoltaic module encapsulants-A comparative study. *Sol. Energy Mater. Sol. Cells* **2013**, *116*, 203−218.

(20) Flory, P. J.; Rehner, J., Jr. Statistical theory of chain configuration and physical properties of high polymers. I. Rubberlike elasticity. II. Swelling. *Ann. N. Y. Acad. Sci.* **1943**, *44*, 419−429.

(21) Dikland, H. G.; Van Duin, A. Miscibility of EPM-EPDM blends. *Rubber Chem. Technol.* **2003**, *76*, 495−506.

(22) Martin, D. L. Crosslink Density Determinations for Polymeric Materials. RK-TR-70-6, 1970.

(23) El-Sabbaghm, S. H.; Yehia, A. A. Detection of Crosslink Density by Different Methods for Natural Rubber Blended with SBR and NBR. *Egypt. J. Solids* **2007**, *2*, 157−173.

(24) Sombatsompop, N. Practical concerns regarding the use of the Mooney-Rivlin equation to assess degree of crosslinking of swollen rubber vulcanisates. *Polym. Polym. Compos.* **1999**, *1*, 41−44.

(25) Mullins, L.; Tobin, N. R. Stress Softening in Rubber Vulcanizates.I. use of a Strain Amplification Factor to Describe Elastic Behavior of Filler-Reinforced Vulcanized Rubber. *J. Appl. Polym. Sci.* **1965**, *9*, 2993−3009.

(26) Mauri, M.; Mauri, L.; Causin, V.; Simonutti, R. A method based on time domain nuclear magnetic resonance for the forensic differentiation of latex gloves. *Anal. Methods* **2011**, *3*, 1802−1809.

(27) Saalwaechter, K. Proton multiple-quantum NMR for the study of chain dynamics and structural constraints in polymeric soft materials. *Prog. Nucl. Magn. Reson. Spectrosc.* **2007**, *51*, 1−35.

(28) Polgar, L. M.; Kingma, A.; Roelfs, M.; van Essen, M.; van Duin, M.; Picchioni, F. Kinetics of cross-linking and de-cross-linking of EPM rubber with thermoreversible Diels-Alder chemistry. *Eur. Polym. J.* **2017**, *90*, 150−161.

(29) Heuert, U.; Knorgen, M.; Menge, H.; Scheler, G.; Schneider, H. New aspects of transversal H-1-NMR relaxation in natural rubber vulcanizates. *Polym. Bull.* **1996**, *37*, 489−496.

(30) Litvinov, V. M.; Barendswaard, W.; van Duin, M. The density of chemical crosslinks and chain entanglements in unfilled EPDM vulcanizates as studied with low resolution, solid state H-1 NMR. *Rubber Chem. Technol.* **1998**, *71*, 105−118.

(31) Dibbanti, M. K.; Mauri, M.; Mauri, L.; Medaglia, G.; Simonutti, R. Probing small network differences in sulfur-cured rubber compounds by combining nuclear magnetic resonance and swelling methods. *J. Appl. Polym. Sci.* **2015**, *132*, 42700.

(32) Magusin, P. C. M. M.; Orza, R. A.; Litvinov, V. M.; van Duin, M.; Saalwächter, K. *NMR Spectroscopy of Polymers: Innovative Strategies for Complex Macromolecules*; American Chemical Society: 2011; Vol. *1077*, pp 207−220.

(33) Chasse, W.; Lopez Valentin, J.; Genesky, G. D.; Cohen, C.; Saalwaechter, K. Precise dipolar coupling constant distribution analysis in proton multiple-quantum NMR of elastomers. *J. Chem. Phys.* **2011**, *134*, 044907.

(34) Faber, M.; Hofman, A. H.; Polushkin, E.; van Ekenstein, G. A.; Seitsonen, J.; Ruokolainen, J.; Loos, K.; ten Brinke, G. Hierarchical Self-Assembly in Supramolecular Double-Comb Diblock Copolymer Complexes. *Macromolecules* **2013**, *46*, 500−517.

(35) Hofman, A. H.; Reza, M.; Ruokolainen, J.; ten Brinke, G.; Loos, K. Hierarchical Self-Assembly of Symmetric Supramolecular Double-Comb Diblock Copolymers: a Comb Density Study. *Macromolecules* **2014**, *47*, 5913−5925.

(36) Yarusso, D. J.; Cooper, S. L. Microstructure of Ionomers - Interpretation of Small-Angle X-Ray-Scattering Data. *Macromolecules* **1983**, *16*, 1871−1880.

(37) Wouters, M. E. L.; Litvinov, V. M.; Binsbergen, F. L.; Goossens, J. G. P.; van Duin, M.; Dikland, H. G. Morphology of ethylene-

DOI: 10.1021/acs.macromol.7b01541
Macromolecules 2017, 50, 8955−8964

propylene copolymer based ionomers as studied by solid state NMR and small angle X-ray scattering in relation to some mechanical properties. *Macromolecules* **2003**, *36*, 1147−1156.
(38) Hertz, D. L. Theory and Practice of Vulcanization. *Elastomerics* **1984**, *11*, 17−21.
(39) Sekkar, V. Comparison Between Crosslink Densities Derived from Stress-Strain Data and Theoretically Data Evaluated Through the alpha-Model Approach for a Polyurethane Network System Based on Hydroxyl Terminated Polybutadiene and Isophorone-Diisocyanate. *J. Appl. Polym. Sci.* **2010**, *117*, 920−925.
(40) Saleesung, T.; Reichert, D.; Saalwaechter, K.; Sirisinha, C. Correlation of crosslink densities using solid state NMR and conventional techniques in peroxide-crosslinked EPDM rubber. *Polymer* **2015**, *56*, 309−317.
(41) Twardowski, T.; Kramer, O. Elastic Contributions from Chain Entangling and Chemical Cross-Links in Elastomer Networks in the Small-Strain Limit. *Macromolecules* **1991**, *24*, 5769−5771.
(42) Di Lorenzo, F.; Seiffert, S. Nanostructural heterogeneity in polymer networks and gels. *Polym. Chem.* **2015**, *6*, 5515−5528.
(43) Shibayama, M. Universality and specificity of polymer gels viewed by scattering methods. *Bull. Chem. Soc. Jpn.* **2006**, *79*, 1799−1819.
(44) Falender, J. R.; Yeh, G. S. Y.; Mark, J. E. Effect of Chain-Length Distribution on Elastomeric Properties 0.1. Comparisons between Random and Highly Non-Random Networks. *J. Am. Chem. Soc.* **1979**, *101*, 7353−7356.
(45) Pan, S. J.; Mark, J. E. Model Networks of End-Linked Polydimethylsiloxane Chains. 15. Spatially Heterogeneous Networks Containing Domains of very High Crosslink Density. *Polym. Bull.* **1982**, *7*, 553−559.
(46) van Bevervoorde-Meilof, E. W. E.; van Haeringen-Trifonova, D.; Vancso, G. J.; Van der Does, L.; Bantjes, A.; Noordermeer, J. W. M. Cross-link Clusters: reality or fiction? A review of the state of the art, enlarged with recent AFM-data. *Kautsch. Gummi Kunstst* **2000**, *7*−*8*, 426−432.
(47) Gonzalez, L.; Rodriguez, A.; Valentin, J. L.; Marcos-Fernandez, A.; Posadas, P. Conventional and efficient crosslinking of natural rubber - Effect of heterogeneities on the physical properties. *Kautsch. Gummi Kunstst.* **2005**, *12*, 638−643.
(48) Burton, B. L.; Bertram, J. L. Polymer network architecture: Molecular scale. In *Polymer Toughening*; Arends, C. B., Ed.; Marcel Dekker: New York, 1996; pp 350−352.
(49) Chen, Y.; Xu, C. Stress-Strain Behaviors and Crosslinked Networks Studies of Natural Rubber-Zinc Dimethacrylate Composites. *J. Macromol. Sci., Part B: Phys.* **2012**, *51*, 1384−1400.
(50) Hofmann, W. *Rubber Technology Handbook*; Hanser Publishers: Münich, 1989.
(51) Zhao, F.; Bi, W.; Zhao, S. Influence of Crosslink Density on Mechanical Properties of Natural Rubber Vulcanizates. *J. Macromol. Sci., Part B: Phys.* **2011**, *50*, 1460−1469.
(52) Boye, W. M. Utilizing coagents in the electron beam cure of elastomers. *Rubber World* **2009**, *1*, 38−44.
(53) Nunes, R. W.; Martin, J. R.; Johnson, J. F. Influence of Molecular-Weight and Molecular-Weight Distribution on Mechanical-Properties of Polymers. *Polym. Eng. Sci.* **1982**, *22*, 205−228.

DOI: 10.1021/acs.macromol.7b01541
Macromolecules 2017, 50, 8955−8964